

## MIT Open Access Articles

*AlGaN/GaN HEMT With 300-GHz  $f_{\max}$* 

The MIT Faculty has made this article openly available. **Please share** how this access benefits you. Your story matters.

**Citation:** Chung, J.W. et al. "AlGaN/GaN HEMT With 300-GHz  $f_{\max}$ ." IEEE Electron Device Letters 31.3 (2010): 195–197. © Copyright 2010 IEEE

**As Published:** <http://dx.doi.org/10.1109/LED.2009.2038935>

**Publisher:** Institute of Electrical and Electronics Engineers (IEEE)

**Persistent URL:** <http://hdl.handle.net/1721.1/78683>

**Version:** Final published version: final published article, as it appeared in a journal, conference proceedings, or other formally published context

**Terms of Use:** Article is made available in accordance with the publisher's policy and may be subject to US copyright law. Please refer to the publisher's site for terms of use.



# AlGaIn/GaN HEMT With 300-GHz $f_{\max}$

Jinwook W. Chung, William E. Hoke, Eduardo M. Chumbes, *Member, IEEE*, and Tomás Palacios, *Member, IEEE*

**Abstract**—We report on a gate-recessed AlGaIn/GaN high-electron mobility transistor (HEMT) on a SiC substrate with a record power-gain cutoff frequency ( $f_{\max}$ ). To achieve this high  $f_{\max}$ , we combined a low-damage gate-recess technology, scaled device geometry, and recessed source/drain ohmic contacts to simultaneously enable minimum short-channel effects (i.e., high output resistance  $R_{ds}$ ) and very low parasitic resistances. A 60-nm-gate-length HEMT with recessed AlGaIn barrier exhibited excellent  $R_{ds}$  of  $95.7 \Omega \cdot \text{mm}$ ,  $R_{on}$  of  $1.1 \sim 1.2 \Omega \cdot \text{mm}$ , and  $f_{\max}$  of 300 GHz, with a breakdown voltage of  $\sim 20$  V. To the authors' knowledge, the obtained  $f_{\max}$  is the highest reported to date for any nitride transistor. The accuracy of the  $f_{\max}$  value is verified by small signal modeling based on carefully extracted S-parameters.

**Index Terms**—AlGaIn, GaN, gate recess, high-electron mobility transistor (HEMT), maximum oscillation frequency ( $f_{\max}$ ), recessed ohmic, short-channel effects, SiC substrate.

## I. INTRODUCTION

GaN-BASED high-electron mobility transistors (HEMTs) have become one of the prime candidates for solid-state power amplifiers at frequencies above 30 GHz. With its unique combination of high electron velocity ( $v_{\text{peak}} \sim 2.5 \times 10^7$  cm/s) and high breakdown electric field ( $\sim 3.3$  MV/cm), these devices have already shown excellent performance, including output power densities in excess of 10 W/mm at 40 GHz [1] and more than 2 W/mm at 80.5 GHz [2], far surpassing other technologies (e.g., Si, GaAs, and InP).

In spite of the great progress in performance achieved during the last few years, there are still several important issues that need to be overcome to further increase the performance of GaN HEMTs at millimeter-wave frequencies (30–300 GHz). One of the key challenges to achieve high-gain millimeter-wave power amplification is to increase the maximum power-gain cutoff frequency ( $f_{\max}$ ).  $f_{\max}$  is the maximum frequency at which the transistor still provides a power gain and can be expressed as [3]

$$f_{\max} \approx \frac{f_T}{2\sqrt{(R_i + R_s + R_g)/R_{ds} + (2\pi f_T)R_g C_{gd}}} \quad (1)$$

where  $f_T$  is the current-gain cutoff frequency and  $C_{gd}$  is the gate–drain (depletion region) capacitance, while  $R_i$ ,  $R_s$ ,  $R_g$ ,

Manuscript received October 26, 2009; revised December 5, 2009. First published January 29, 2010; current version published February 24, 2010. This work was supported in part by the Office of Naval Research MINE MURI and Young Investigator Programs monitored by Dr. Dietrich and Dr. Maki. The work of J. W. Chung was supported by the Korea Foundation for Advanced Studies. The review of this letter was arranged by Editor G. Meneghesso.

J. W. Chung and T. Palacios are with the Microsystems Technology Laboratories, Massachusetts Institute of Technology, Cambridge, MA 02139 USA (e-mail: wilchung@mit.edu; tpalacios@mit.edu).

W. E. Hoke and E. M. Chumbes are with the Raytheon Integrated Defense Systems, Andover, MA 01810 USA (e-mail: William\_E\_Hoke@raytheon.com; Eduardo\_M\_Chumbes@raytheon.com).

Color versions of one or more of the figures in this letter are available online at <http://ieeexplore.ieee.org>.

Digital Object Identifier 10.1109/LED.2009.2038935

and  $R_{ds}$  represent the gate-charging, source, gate, and output resistance, respectively. To maximize  $f_{\max}$ , each parameter needs to be carefully optimized.  $f_T$ , for example, has been extensively studied and greatly improved by reducing the gate length to 30 nm [4]. However, despite its great importance, other parasitic components have been barely investigated. In this letter, we describe new design features to reduce both short-channel effects ( $R_{ds}$  and  $C_{gd}$ ) and parasitic resistances ( $R_i$ ,  $R_s$ , and  $R_g$ ) to achieve a very high  $f_{\max}$ .

In field-effect transistors, the short-channel effects play an important role in the high-frequency characteristics [5]. However, improvement of the short-channel effects has been seldom a path to improve the high-frequency performance in GaN HEMTs. In this letter, we applied a low-damage gate-recess technology to effectively suppress the short-channel effects. The resultant HEMT showed excellent output characteristics with a very high  $R_{ds}$  of  $95.7 \Omega \cdot \text{mm}$ , small  $C_{gd}$  of  $42.6$  fF/mm, and good pinchoff behavior. Also, the closer gate-to-channel distance helped reduce  $R_i$ , which is proportional to the charging time of the gate–source capacitance ( $C_{gs}$ ).

The parasitic resistances are also very important in that they can significantly degrade the frequency performance [6], [7]. To minimize them, we combined a short source-to-drain distance and recessed source/drain ohmic contacts [8]. Combination of  $1.1$ - $\mu\text{m}$  source-to-drain distance and optimized ohmic contact resistance ( $R_c$ ) of  $0.15 \Omega \cdot \text{mm}$  resulted in extremely low  $R_{on}$  of  $1.1 \sim 1.2 \Omega \cdot \text{mm}$  and a knee voltage of only 2 V. In addition, a T-shaped gate was fabricated to reduce  $R_g$ . Finally, our 60-nm-gate-length AlGaIn/GaN HEMT exhibited a record  $f_{\max}$  of 300 GHz, which, to the best of our knowledge, is the highest in any nitride transistor.

## II. DEVICE FABRICATION

The AlGaIn/GaN transistor structure was grown on a SiC substrate by molecular beam epitaxy at Raytheon IDS. This structure produced a 2DEG with a total charge density of  $8 \times 10^{12}/\text{cm}^2$  and electron mobility of  $2200 \text{ cm}^2/\text{V} \cdot \text{s}$  as measured on unpassivated samples using van der Pauw structures at room temperature. This mobility and charge density translate to a 2DEG sheet resistance of  $356 \Omega/\text{sq}$ .

Device fabrication began with mesa isolation using a  $\text{Cl}_2/\text{BCl}_3$  plasma-based dry etch. Then, recessed ohmic technique was used to reduce the ohmic contact resistances. First, source and drain regions with a  $1.1$ - $\mu\text{m}$  separation [Fig. 1(a)] are defined by photolithography, and the AlGaIn barrier is slowly etched using a low-power electron cyclotron resonance reactive ion etching (ECR-RIE) with  $\text{Cl}_2/\text{BCl}_3$  gas mixture. To minimize the damage induced by ion bombardment, RF bias was kept low ( $\sim 75$  V), while ECR power was set to achieve an etch rate of  $1 \text{ nm}/\text{min}$  ( $\sim 100$  W). After the recess,

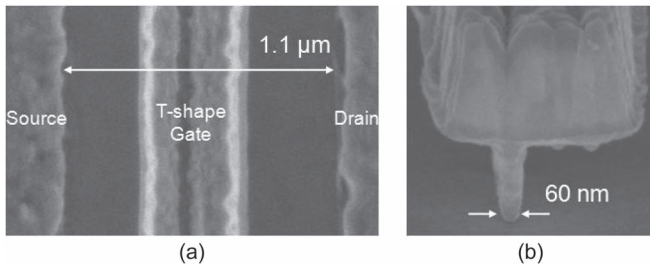


Fig. 1. (a) Plan-view SEM image of the fabricated HEMTs. The source-to-drain distance in this device is 1.1  $\mu\text{m}$ . (b) A cross-sectional SEM image of the 60-nm T-shaped gate.

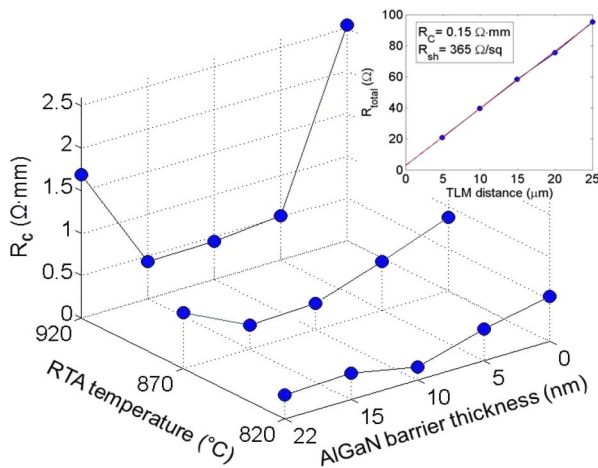


Fig. 2. Measured contact resistance ( $R_c$ ) as function of RTA temperature and remaining AlGaIn barrier thickness. The optimum  $R_c$  of 0.15  $\Omega \cdot \text{mm}$  was obtained at the 10-nm AlGaIn barrier after annealing at 820  $^\circ\text{C}$  for 30 s in  $\text{N}_2$  ambient. The sheet resistance ( $R_{sh}$ ) was kept almost constant ( $\sim 360 \Omega/\text{sq}$ ) in all cases. In the devices with no remaining AlGaIn barrier under the contacts, the ohmic contact is formed laterally between the annealed metals and the 2DEG in the unrecessed AlGaIn/GaN access region [9].

a Ti/Al/Ni/Au metal stack was deposited, followed by rapid thermal annealing (RTA) for 30 s in the  $\text{N}_2$  atmosphere. RTA temperature and remaining AlGaIn barrier thickness were experimentally optimized to have the lowest contact resistance, as shown in Fig. 2. The best condition among the range that we explored was found at 820  $^\circ\text{C}$  with a 10-nm AlGaIn barrier yielding an  $R_c$  of 0.15  $\Omega \cdot \text{mm}$ , which is one of the lowest contact resistances reported in the literature.

Electron-beam lithography was applied to define a T-shaped gate using a trilayer resist stack made of PMMA/Copolymer/PMMA. For the gate recess, we utilized the same technique as the recessed ohmic. We did not observe any degradation in the source-to-drain current after the recess [10]. Following the gate recess, a Ni/Au/Ni metal stack was deposited for the gate contact. The 60-nm physical gate length was confirmed by scanning electron microscope (SEM), as shown in Fig. 1(b). The devices were not passivated.

### III. RESULTS AND DISCUSSION

Fig. 3 shows the dc characteristics of the fabricated 60-nm gate-recessed AlGaIn/GaN HEMT. The short source-to-drain distance in combination with the low ohmic contact resistance allowed a very low ON-resistance of 1.1  $\sim 1.2 \Omega \cdot \text{mm}$  and a knee voltage of only 2 V. Also, the short-channel effects were

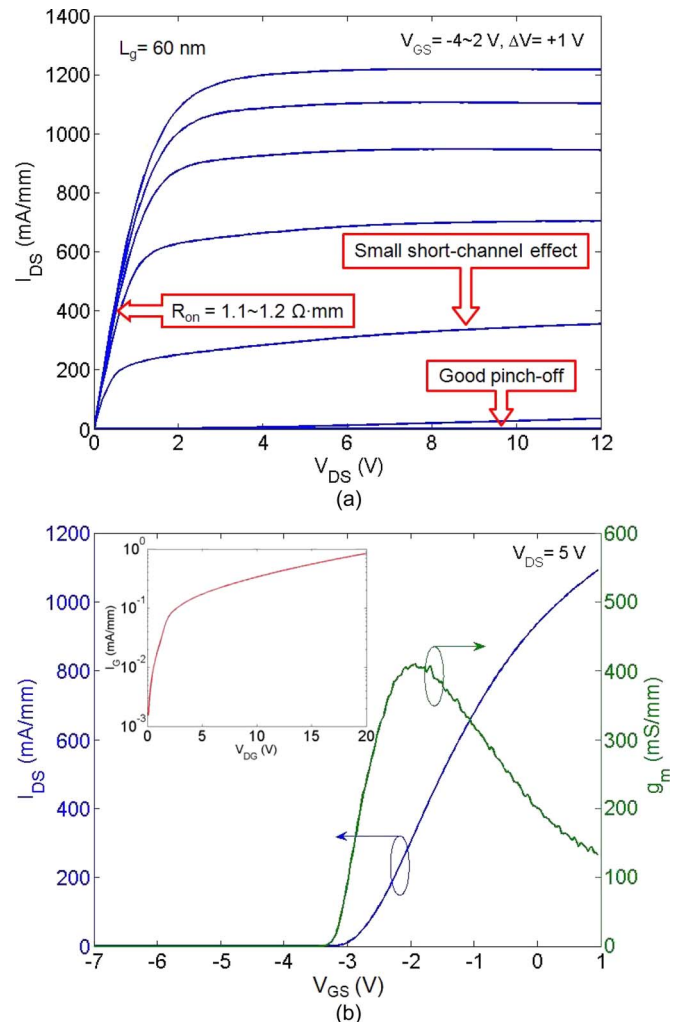


Fig. 3. (a) DC characteristics of the 60-nm gate-recessed AlGaIn/GaN HEMT. (a) Output characteristics with a good pinchoff, low  $R_{on}$  of 1.1  $\sim 1.2 \Omega \cdot \text{mm}$ , knee voltage of just 2 V, and high output resistance (small short-channel effect). (b) Transfer characteristics at  $V_{DS} = 5 \text{ V}$  and (inset) the two-terminal gate-drain breakdown voltage of  $\sim 20 \text{ V}$  defined at a 1-mA/mm reverse gate current.

effectively suppressed by the gate-recess technology as demonstrated by the high output resistance ( $R_{ds} = 95.7 \Omega \cdot \text{mm}$ ) and the good pinchoff ( $I_{on}/I_{off} \sim 5 \times 10^3$ ). This improvement is mainly attributed to better gate control over the channel by improved aspect ratio between the gate length and AlGaIn barrier thickness. The maximum drain current at  $V_{GS} = 2 \text{ V}$  was 1.2 A/mm, and the peak extrinsic transconductance at  $V_{DS} = 5 \text{ V}$  was 410 mS/mm. The two-terminal gate-drain breakdown voltage was  $\sim 20 \text{ V}$ . As part of our on-going work, we are currently developing high- $k$  gate dielectric [11] to minimize the gate leakage as well as to allow even more aggressive gate recesses for improved gate modulation efficiency.

The RF performance of these devices was characterized from 0.45 to 50 GHz using an Agilent Technologies N5230A network analyzer. The system was calibrated with a short-open-load-through calibration standard. The calibration was verified by insuring that both  $S_{12}$  and  $S_{21}$  of the through standard are less than  $\pm 0.01 \text{ dB}$  and that both  $S_{11}$  and  $S_{22}$  are less than  $-45 \text{ dB}$  within the measured frequency range after the calibration [5]. On-wafer open and short patterns were used to

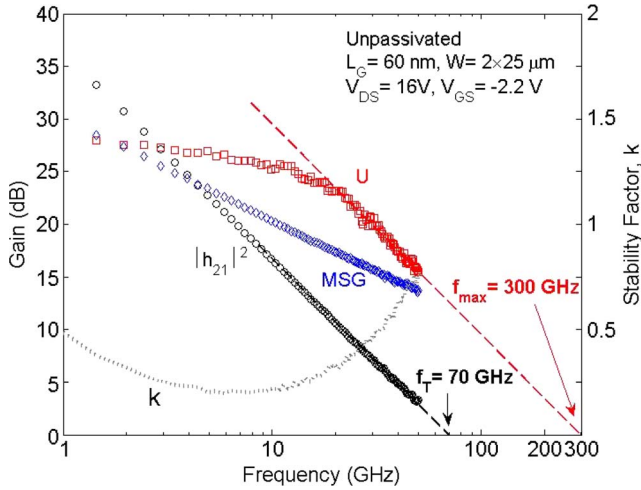


Fig. 4. RF performance of unpassivated 60-nm-gate-length HEMT showing  $f_T = 70$  GHz and  $f_{\max} = 300$  GHz. The  $f_T$  and  $f_{\max}$  values are extrapolated following a  $-20$  dB/dec ideal decrease with frequency.

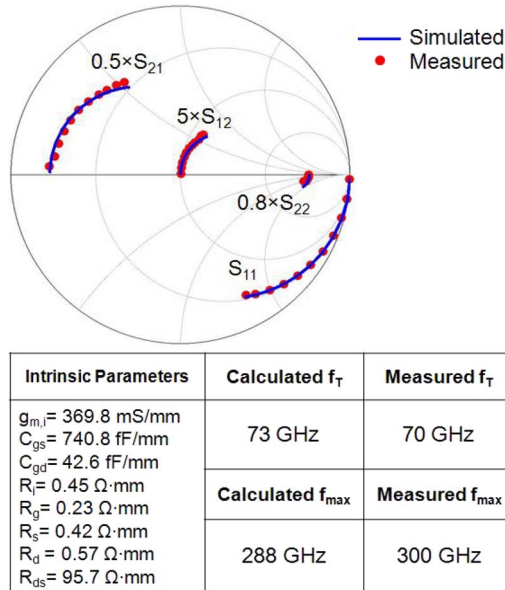


Fig. 5. (Top) Comparison of simulated and measured S-parameters at  $V_{DS} = 16$  V and  $V_{GS} = -2.2$  V. (Bottom) Table shows the extracted intrinsic parameters and calculated  $f_T/f_{\max}$ .

subtract the effect of parasitic pad capacitances and inductances from the measured S-parameters [12]. Due to the effect of the pad capacitances, the  $f_T$  and  $f_{\max}$  values calculated from the extrinsic S-parameters were 10% lower than the intrinsic values. The reproducibility error in our measurements due to the calibration was less than 5%. Fig. 4 shows  $|h_{21}|^2$  and Mason's unilateral gain  $U$  against frequency for the 60-nm-gate-length device at  $V_{DS} = 16$  V and  $V_{GS} = -2.2$  V. An  $f_T$  of 70 GHz and a record  $f_{\max}$  of 300 GHz were obtained by extrapolating measured data with a slope of  $-20$  dB/dec using a least-square fit. For comparison, the highest  $f_{\max}$  reported so far in nitride transistors was 251 GHz in 4-nm barrier AlGaIn/GaN HEMTs with 60-nm gate length [13]. The  $f_T/f_{\max}$  values are confirmed through S-parameter simulations in the 0.45–50 GHz range [14], as shown in Fig. 5. The small discrepancy between measurements and simulations (i.e., 300 GHz versus 288 GHz)

could originate from incomplete small-signal model or (1) used in this letter. The relatively low  $f_T$  value is due to a combination of a lower than expected intrinsic RF transconductance  $g_{m,i} \sim 370$  mS/mm (versus the calculated intrinsic dc transconductance of  $\sim 490$  mS/mm) and the high gate-to-source capacitance ( $C_{gs}$ ) resulting from the extended effective gate length ( $L_{\text{eff}} = (C_{gs} \cdot d_{\text{AlGaIn}})/\epsilon \approx 100$  nm) at the large drain voltage used during the measurements ( $V_{DS} = 16$  V).

#### IV. CONCLUSION

We have reported  $L_g = 60$  nm gate-recessed AlGaIn/GaN HEMTs on SiC substrate having a record  $f_{\max}$  of 300 GHz. Owing to the low-damage gate recess, short source-to-drain distance, and recessed ohmic contacts, the short-channel effects, as well as parasitic resistances, were effectively suppressed. The fabrication technology and the record  $f_{\max}$  reported in this letter demonstrate the unsurpassed potential of GaN transistors for millimeter- and submillimeter-wave power amplifiers.

#### REFERENCES

- [1] T. Palacios, A. Chakraborty, S. Rajan, C. Poblenz, S. Keller, S. P. DenBaars, J. S. Speck, and U. K. Mishra, "High-power AlGaIn/GaN HEMTs for Ka-band applications," *IEEE Electron Device Lett.*, vol. 26, no. 11, pp. 781–783, Nov. 2005.
- [2] M. Micovic, A. Kurdoghlian, P. Hashimoto, M. Hu, M. Antcliff, P. J. Willadsen, W. S. Wong, R. Bowen, I. Milosavljevic, A. Schmitz, M. Wetzel, and D. H. Chow, "GaN HFET for W-band power applications," in *IEDM Tech. Dig.*, 2006, pp. 425–427.
- [3] S. M. Sze, *Physics of Semiconductor Devices*. New York: Wiley, 1981, pp. 342–343.
- [4] M. Higashiwaki, T. Mimura, and T. Matsui, "30-nm-gate AlGaIn/GaN heterostructure field-effect transistors with a current-gain cutoff frequency of 181 GHz," *Jpn. J. Appl. Phys.*, vol. 45, no. 42, pp. L1111–L1113, Oct. 2006.
- [5] D.-H. Kim and J. A. del Alamo, "30-nm InAs pseudomorphic HEMTs on an InP substrate with a current-gain cutoff frequency of 628 GHz," *IEEE Electron Device Lett.*, vol. 29, no. 8, pp. 830–833, Aug. 2008.
- [6] P. J. Tasker and B. Hughes, "Importance of source and drain resistance to the maximum  $f_T$  of millimeter-wave MODFETs," *IEEE Electron Device Lett.*, vol. 10, no. 7, pp. 291–293, Jul. 1989.
- [7] Nidhi, T. Palacios, A. Chakraborty, S. Keller, and U. K. Mishra, "Study of impact of access resistance on high-frequency performance of AlGaIn/GaN HEMTs by measurements at low temperatures," *IEEE Electron Device Lett.*, vol. 27, no. 11, pp. 877–880, Nov. 2006.
- [8] D. Buttari, A. Chini, G. Meneghesso, E. Zanoni, B. Moran, S. Heikman, N. Q. Zhang, L. Shen, R. Coffie, S. P. DenBaars, and U. K. Mishra, "Systematic characterization of  $\text{Cl}_2$  reactive ion etching for improved ohmics in AlGaIn/GaN HEMTs," *IEEE Electron Device Lett.*, vol. 23, no. 2, pp. 76–78, Feb. 2002.
- [9] L. Wang, D.-H. Kim, and I. Adesida, "Direct contact mechanism of ohmic metallization to AlGaIn/GaN heterostructures via ohmic area recess etching," *Appl. Phys. Lett.*, vol. 95, no. 17, p. 172107, Oct. 2009.
- [10] J. W. Chung, O. I. Saadat, J. M. Tirado, X. Gao, S. Guo, and T. Palacios, "Gate-recessed InAlN/GaN HEMTs on SiC substrate with  $\text{Al}_2\text{O}_3$  passivation," *IEEE Electron Device Lett.*, vol. 30, no. 9, pp. 904–906, Sep. 2009.
- [11] O. I. Saadat, J. W. Chung, E. L. Piner, and T. Palacios, "Gate-first AlGaIn/GaN HEMT technology for high-frequency applications," *IEEE Electron Device Lett.*, vol. 30, no. 12, pp. 1254–1256, Dec. 2009.
- [12] H. Matsuzaki, T. Maruyama, T. Koasugi, H. Takahashi, M. Tokumitsu, and T. Enoki, "Lateral scale down of InGaAs/InAs composite-channel HEMTs with tungsten-based tiered ohmic structure for 2-S/mm  $g_m$  and 500-GHz  $f_T$ ," *IEEE Trans. Electron Devices*, vol. 54, no. 3, pp. 378–384, Mar. 2007.
- [13] M. Higashiwaki, T. Mimura, and T. Matsui, "AlGaIn/GaN heterostructure field-effect transistors on 4H-SiC substrates with current-gain cutoff frequency of 190 GHz," *Appl. Phys. Express*, vol. 1, p. 021103, Feb. 2008.
- [14] F. Mieville, "Suitability of GaN HEMTs for digital electronics," M.S. thesis, MIT, Cambridge, MA, 2008.